Biased Random Walk by Stochastic Fluctuations of Chemoattractant-Receptor Interactions at the Lower Limit of Detection

Peter J. M. van Haastert* and Marten Postma†
*Department of Molecular Cell Biology, University of Groningen, 9751NN Haren, The Netherlands; and †Department of Physiology, Development and Neuroscience, Cambridge University, Cambridge CB2 3DY, United Kingdom

ABSTRACT Binding of ligand to its receptor is a stochastic process that exhibits fluctuations in time and space. In chemotaxis, this leads to a noisy input signal. Therefore, in a gradient of chemoattractant, the cell may occasionally experience a "wrong" gradient of occupied receptors. We obtained a simple equation for P_{pos}, the probability that half of the cell closest to the source of chemoattractant has higher receptor occupancy than the opposite half of the cell. P_{pos} depends on four factors, the gradient property $\nabla C/\sqrt{C}$, the receptor characteristic R_t/K_D, a time-averaging constant I, and nonreceptor noise σ_B. We measured chemotaxis of *Dictyostelium* cells to known shallow gradients of cAMP and obtained direct estimates for these constants. Furthermore, we observed that in shallow gradients, the measured chemotaxis index is correlated with P_{pos}, which suggests that chemotaxis in shallow gradients is a pure biased random walk. From the observed chemotaxis and derived time-averaging constant, we deduce that the gradient transducing second messenger has a lifetime of 2–8 s and a diffusion rate constant of $\sim 1\ \mu m^2/s$. Potential candidates for such second messengers are discussed.

INTRODUCTION

Chemotaxis is a pivotal response of many cell types to external spatial cues. It plays important roles in diverse functions such as finding nutrients in prokaryotes, forming multicellular structures in protozoa, tracking bacterial infections in neutrophils, and organizing the embryonic cells in metazoa (1–3). Chemotaxis is achieved by coupling gradient sensing to basic cell movement. Whereas prokaryotes are too small ($\sim 1\ \mu m$) to sense spatial gradients and therefore rely on temporal changes of the chemoattractant concentration, eukaryotes are large enough (10–20 μm) to process spatial gradients as well as temporal gradients. Prokaryotes adjust their tumbling frequency in response to temporal changes of the chemoattractant concentration (4,5). In eukaryotes, the difference in receptor occupation across the cell body leads to pseudopod extension directed toward the higher concentration in a chemical gradient (6,7).

In *Dictyostelium* cells, extracellular cAMP functions as chemoattractant that is detected by specific G-protein coupled surface receptors. Cells are able to sense the cAMP gradient over a wide range of concentrations from 0.1 nM to 10 μM, with concentration differences of only 1–5% across the cell (8,9). A significant chemotactic response is induced at a threshold close to 0.5 nM cAMP with a gradient of 9%. *Dictyostelium* cells have ~40,000 cAMP receptors with a dissociation constant (K_D) that is ~100 nM, implying that at threshold concentrations, ~200 receptors are occupied in total. Since the cells are ~10 μm in size and receptors are distributed homogeneously around the cell (10), at the threshold gradient the front half of the cell has ~5 more occupied receptors than the back half of the cell. Binding of cAMP to the receptor is a stochastic process and therefore fluctuates in time, and consequently will vary in space as well. At these low threshold concentrations, the receptor occupancy statistics can be approximated by a Poisson distribution (11). The standard deviation in receptor occupancy then equals the square root of the mean receptor occupancy. Thus at threshold chemotaxis with an average occupancy of ~200 receptors/cell, the fluctuation around the mean is ~14 receptors/cell, whereas the difference between front and back half of the cell is only ~5 receptors/cell. Such fluctuations of input signals have been observed by single molecule imaging of cAMP-binding to living *Dictyostelium* cells (11). How does the chemotactic system obtain reliable information regarding the cAMP gradient with these noisy inputs? This question is critical, because the downstream gain present in chemotactic signaling will amplify small changes in cAMP concentration, and such systems will therefore amplify the noise as well.

Berg and Purcell (12), and more recently Bialek and Setayeshgar (13), have shown that statistical fluctuations limit the precision by which a cell, in a given time T, can determine the concentration of a chemoattractant in the surrounding medium. They have shown that the transduction time acts as time averaging the input signal, which will reduce transducer noise. For leukocytes, a stochastic model has been proposed based on the small fluctuations in turning direction at the front of the cell, which has an intrinsic polarity axis (14–16). However, *Dictyostelium* and many other amoeboid cells are not polarized in buffer. At these conditions, the direction in which a new pseudopod is extended is only slightly correlated with the direction of a previous

Submitted January 12, 2007, and accepted for publication April 16, 2007.

Address reprint requests to Peter J. M. van Haastert, Dept. of Molecular Cell Biology, University of Groningen, Kerklaan 30, 9751NN Haren, The Netherlands. Tel.: 31-503-634172; Fax: 31-503-634165; E-mail: P.J.M.van.Haastert@rug.nl.

Editor: Jennifer Linderman.

0006-3495/07/09/1787/10 $2.00

doi: 10.1529/biophysj.107.104356

pseudopod, and cell tracks essentially have the characteristics of a random walk (17–19). In a gradient of chemoattractant, pseudopodia can still be formed in all directions, but it occurs more frequently in the direction of the gradient. In such a biased random walk, noise is an intrinsic property of chemoreception.

We have analyzed *Dictyostelium* chemotaxis in shallow cAMP gradients where noise is a more dominant component of the signal transduction cascade, and derived an equation for the probability that the cell experience a higher receptor occupancy at the side of the cell closest to the chemoattractant source than at the opposite side of the cell. This probability is called P_{pos}, and includes experimental estimates of the noise and time-averaging period. We observed that the measured chemotaxis index is directly proportional to P_{pos}, suggesting that chemotaxis in shallow gradients is a pure biased random walk.

MATERIALS AND METHODS

Strains and growth conditions

The wild-type *Dictyostelium discoideum* strain AX3 was used in all experiments. Cells were grown in shaking culture in HG5 medium (contains per liter: 14.3 g oxoid peptone, 7.15 g bacto yeast extract, 1.36 g $Na_2HPO_4{\cdot}12H_2O$, 0.49 g KH_2PO_4, 10.0 g glucose) at a density between 5×10^5 and 6×10^6 cells/ml. Cells were harvested by centrifugation for 3 min at 300 g, washed in phosphate buffer (PB) (10 mM KH_2PO_4/Na_2HPO_4, pH 6.5) and starved in PB in 6-well plates (Nunc) for 5 h. Cells were then resuspended in PB, centrifuged and washed once in PB, and resuspended in PB at a density of 5×10^6 cells/ml.

Chemotaxis

Three assays were used to quantify chemotaxis. In the pipette assay, a droplet of ~0.5 ml of the cell suspension was placed on a microscope glass slide. Cells were allowed to adhere to that glass for 15 min, and then cells were stimulated with a micropipette. The Eppendorf femtotip, filled with different concentrations of cAMP, was placed just above the glass surface and cAMP was released at a pressure of 25 hPa. Cells were monitored by phase contrast microscopy and images were captured every 10 s during 20 min. The formation of the cAMP gradient was deduced from experiments in which the fluorescent dye Lucifer yellow was mixed with cAMP in the pipette. The fluorescence intensity at different distances of the pipette was recorded using a confocal fluorescent microscope in pixel elements (0.404×0.404 μm), and calibrated using the fluorescence intensity of a diluted Lucifer Yellow added homogeneously to the bath. The results (data not shown) reveal that the gradient is formed very fast (the time at which half-maximal equilibrium is reached was ~10–20 s), and follows Eq. A1 at distances from the pipette beyond 15 μm. From these experiments, we obtained the portionality constant of Eq. A1, $\alpha = 0.05$.

The second chemotaxis assay employs a modified Zigmond chamber (20). On a microscope slide, a glass bridge of 24×2 mm was places on top of two supporting glass strips with thickness 0.15 mm. Cells were places under the bridge. A block of agar containing only PB buffer was placed at one side of the bridge, while a block of agar containing cAMP and buffer was placed at the other side. A gradient of cAMP was formed under the bridge. Cells were observed by phase contrast microscopy in an area of 350×270 μm at a distance of 700 μm from the agar block containing cAMP, and images were captured every 10 s during 20 min. The dye bromophenol blue was used to follow the formation of the cAMP gradient (20).

The small population assay was used as the third chemotaxis assay (8,21). Droplets of ~0.1 μl of 5-h starved cells (6×10^6 cells/ml) were placed on nonnutrient hydrophobic agar (11 mMKH2PO4, 2.8 mM Na2HPO4, 7 g/l hydrophobic agar). Chemotaxis toward cAMP was tested by placing a second 0.1 μl droplet, with the indicated concentration of cAMP, next to the droplet of cells. The distance between the droplets, defined by the distance between the center of the cAMP-containing droplet and the closest edge of the cell-containing droplet, was either 250 or 650 μm. The distribution of the cells in the droplet was observed, and scored positive when at least twice as many cells were pressed against the side of the higher cAMP concentration as against the other side of the droplet. Recorded was the fraction of droplets scored positive.

The motile behavior of cells in spatial gradients of cAMP was analyzed using computer-assisted methods previously described (22). Briefly, images of the pipette assay and the modified Zigmond assay were used to determine the contour of the cell and the position of the cell centroid. Chemotactic index, defined as the distance moved in the direction of the cAMP gradient divided by the total distance moved, was computed from the centroid positions for each subsequent image, and averaged for each cell over at least 20 images. Reported were the means and standard error of the means of at least 30 cells from two or three experiments.

RESULTS

Chemotaxis at different gradients of cAMP

Three different assays were used to measure the chemotactic response of *Dictyostelium* cells: a micropipette assay, a modified Zigmond chamber, and the small population assay. The equation for the formation of cAMP gradients around the cell are presented in the Appendix We measured the chemotaxis index (Ψ) toward a pipette with buffer and obtained $\Psi = 0.01 \pm 0.05$ based on $n = 24$ (mean $\pm$ SE), which is statistically equal to zero. The threshold gradient for chemotaxis is defined as the smallest gradient that yields a chemotaxis index that is statistically significant above this value in buffer. With $n = 24$ and $P < 0.01$, the threshold chemotaxis index is close to $\Psi = 0.2$.

We have determined the chemotaxis index of cells at different distances from the pipette, demonstrating that cells exhibit significant chemotaxis as far as 700 μm from a pipette filled with 10^{-4} M cAMP (Fig. 1 *A*). A half-maximal chemotaxis response ($\Psi = 0.5$) is observed at ~300 μm from the pipette. When the pipette contains lower concentrations of cAMP, cells far away from the pipette no longer respond, but closer to the pipette cells still exhibit significant chemotaxis. In the modified Zigmond chamber, cells are deposited under a 2 mm wide glass bridge. A cAMP gradient is formed by placing agar blocks with buffer on one side of the bridge and an agar block with cAMP on the other side (20). Cells are observed at a distance of ~700 μm from the source. Using 1 μM cAMP in the source block, the gradient is 0.5 nM/μm at a mean cAMP concentration of 660 nM, yielding a concentration difference of ~0.7% over the cell length. This gradient induced a chemotaxis index of ~0.7 (Fig. 1 *B*). The chemotaxis index becomes smaller when the cAMP concentration in the source block is reduced. At 10 nM cAMP, the threshold chemotaxis index of ~0.2 is

observed, whereas the chemotaxis index is statistically indistinguishable from zero at a concentration of 1 nM cAMP. The small population assay scores the chemotactic response of a population of cells toward a cAMP source that has been applied at some distance away as a single dose. When the cAMP and *Dictyostelium* droplets are placed close together ($x = 250\ \mu$m), significant chemotaxis is detected at 3–10 nM cAMP in the droplet. A half-maximal response is induced by 30 nM cAMP, whereas the response saturates at 1 μM cAMP in the droplet (Fig. 1 *B*). When the distance between cAMP and cells is increased to $x = 650\ \mu$m, ~100-fold higher cAMP concentrations are required to induce a chemotactic response with similar strength as with $x = 250\ \mu$m.

Table 1 summarizes the experimental conditions of the assays where we observed a threshold chemotaxis of $\Psi = 0.2$. Equations A1–A6 of the Appendix were used to calculate the concentration and spatial gradient around the cell, showing that a threshold chemotactic response can be induced at a 60-fold difference in cAMP concentrations and fourfold difference in spatial gradient, depending on the assay used. The number of occupied receptors per cell was calculated, as well as the difference of occupied receptors between the front and back half of the cell. Chemotaxis can be induced when the difference between the front and back of the cell is as little as five occupied receptors when only 0.3% of the receptors are occupied with cAMP. At higher cAMP concentrations, when ~7% of the receptors are occupied, the difference between the front and back is still only 10 occupied receptors. These experimental data clearly show that threshold chemotaxis can be obtained at different magnitudes of the spatial gradient and absolute concentration, which will be used below to derive estimates of the noise parameters for chemotaxis.

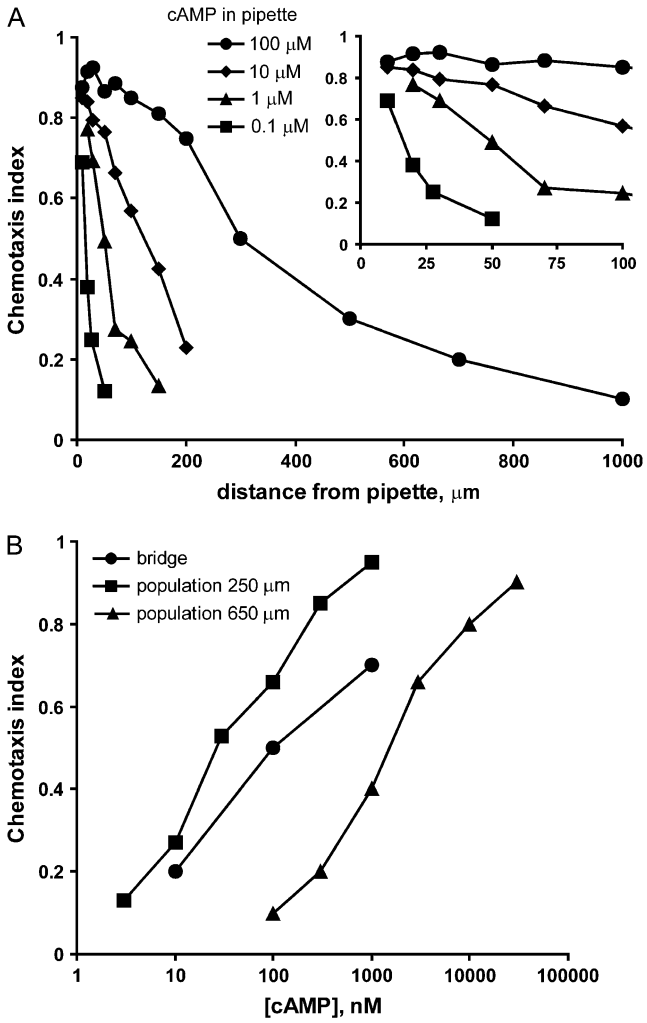

FIGURE 1 Chemotactic activity of *Dictyostelium* cells toward cAMP. (*A*) Cells were stimulated with micropipettes containing different concentrations of cAMP as indicated. (*B*) Chemotaxis with the small population assay at different distances between cells and cAMP as indicated, or with the bridge assay, a modified Zigmond chamber. The results shown are the means of at least three independent experiments.

Receptor noise leading to biased random walk at threshold chemotaxis

The cell measures the cAMP gradient by means of surface cAMP receptors. The input signal is a spatial cAMP gradient, which is detected by the cell as the difference of occupied receptors between the front and back half of the cell, ΔR^*. In shallow gradients (<10% across the cell), ΔR^* is given approximately (see the Appendix A7) by

$$\Delta R^* = \frac{R_t}{4}\frac{\Delta C}{C + K_D}, \tag{1}$$

where ΔC is the cAMP concentration difference between the front and back of the cell, R_t is the number of receptors (40,000/cell), and K_D is the dissociation constant of the receptor (100 nM).

The interaction between cAMP and its receptor has been investigated in vivo by single molecule detection, demonstrating that the interaction is stochastic (11). Random association and dissociation reactions of cAMP-receptor interactions inevitably leads to fluctuations in the number of occupied receptors, and consequently receptor activation is noisy. The noise in the chemotactic system due to fluctuations in receptors occupancy follows binomial statistics, depending on the number of occupied and unoccupied receptors. When the chemotactic system time averages the receptor occupancy over a characteristic sampling time T, the variance of the number of occupied receptors after sampling ($\sigma^2_{R^*_F}$) at low cAMP concentrations ($C < K_D$) is given by (see the Appendix)

$$\sigma^2_{R^*_F} = \frac{R^*}{I}, \tag{2}$$

where I is introduced as the sampling fold, which indicates how often a receptor measures the cAMP concentration in the time T. The sampling fold I is given by

$$I = \frac{T}{2\tau_R}\left[1 - \frac{\tau_R}{T}\left(1 - e^{-\frac{T}{\tau_R}}\right)\right]^{-1}, \tag{3}$$

TABLE 1 Conditions for threshold chemotaxis ($\Psi = 0.2$)

Assay	Condition	C(nM)	∇C(pM/μm)	$\nabla C/C$ (%/10 μm)	R^*	∇R^*
Pipette 0.1 μM cAMP	30 μm	0.17	5.56	33.33	67	5.5
Pipette 1 μM cAMP	100 μm	0.50	5.00	10.00	199	5.0
Pipette 10 μM cAMP	210 μm	2.38	11.34	4.76	930	11.07
Pipette 100 μM cAMP	700 μm	7.14	10.20	1.43	2667	9.52
Small population 250 μm	6 nM	0.62	6.02	9.68	247	5.98
Small population 650 μm	300 nM	1.77	6.59	3.72	696	6.47

The conditions inducing threshold chemotaxis ($\Psi = 0.2$) were deduced from Fig. 1. The concentration C and the spatial gradient ∇C at the cells were calculated using Eqs. A1–A6. R* is the total number of occupied receptors per cell, and ∇R^* is the difference of occupied receptors between the front and back half of the cell.

where at low cAMP concentrations $\tau_R = 1/k_{-1}$, which denotes the lifetime of the cAMP-receptor complex.

Besides noise due to fluctuations in the cAMP-receptor interaction, the system will also contain nonreceptor noise, originating from fluctuations in the second messenger system downstream of the receptor. This nonreceptor noise σ_B will increase the variance and reduce the accuracy by which the spatial gradient can be detected.

The signal/noise ratio (SNR) is then given by

$$SNR = \frac{\Delta R^*}{\sqrt{\sigma_B^2 + \sigma_{R_F^*}^2}} = \frac{\frac{\Delta C R_t}{4K_D}}{\sqrt{\sigma_B^2 + \frac{CR_t}{K_D I}}}. \quad (4)$$

Note that in the absence of nonreceptor noise (i.e., $\sigma_B = 0$) Eq. 4 reduces to

$$SNR = \frac{\Delta C}{\sqrt{C}} \sqrt{\frac{R_t}{16K_D}} \sqrt{I}. \quad (5)$$

Thus, SNR consists of four parts: nonreceptor noise σ_B, the cAMP gradient property $\Delta C/\sqrt{C}$, receptor property $\sqrt{R_t/16K_D}$, and the sampling fold $\sqrt{I}$. The SNR increases, i.e., the gradient is measured more accurately, when nonreceptor noise σ_B is smaller, when the spatial cAMP gradient ΔC is steeper at lower average cAMP concentration C, when the number of receptors R_t or the affinity of the receptors for cAMP K_D^{-1} increase, or when the sampling fold I increases.

Due to stochastic fluctuations of occupied receptors, the front of the cell may occasionally experience a ''wrong'' lower receptor occupancy than the back of the cell. The probability that the cell experiences a net positive signal in the direction of the gradient is called P_{pos} and is given by

$$P_{pos} = P(\Delta R > 0) - P(\Delta R < 0) = Erf[(\mathrm{SNR}/\sqrt{2}], \quad (6)$$

where *Erf* is the error function.

We are especially interested in chemotaxis at threshold gradients, where SNR and P_{pos} are expected to be small. The inset of Fig. 2 reveals that P_{pos} reaches significant values at rather low values of SNR. Thus, the probability that the front of the cell measures a positive gradient is 0.2 at a SNR of 0.15, i.e., when the noise is sevenfold larger than the signal. Furthermore, the figure shows that P_{pos} is linear with SNR for SNR < 0.7 with a slope of $\sqrt{2/\pi}$, i.e., $Erf[(\mathrm{SNR}/\sqrt{2}] \approx \sqrt{2/\pi}\mathrm{SNR}$. We calculated P_{pos} as function of the distance from a pipette with 10^{-4} M cAMP for different values of nonreceptor noise σ_B, sampling fold I, and receptor property R_t/K_D. Fig. 2 shows that with $\sigma_B = 0$ and $I = 1$ (curve *c*), P_{pos} reaches half-maximal value of 0.5 at a distance of ~300 μm from the pipette. At a nonreceptor noise of 10 or 100 (curves *a* and *b*), half-maximal P_{pos} is obtained much closer to the pipette. In contrast, increasing the sampling fold I to 3 or 10 (curves *d* and *e*) leads to a significant increase of P_{pos}, by which cells farther away from the pipette may respond. Increasing the number of receptors R_t or the affinity of the receptor $1/K_D$ has the same effect as increasing the sampling fold: the value of P_{pos} increases by which cells may detect the cAMP gradient more easily. The observed values for the chemotaxis index Ψ are also presented in Fig. 2, demonstrating that the experimental data exhibit the same distance-dependency as the calculated curves for P_{pos}. This is especially valid far away from the pipette. Closer to the pipette within a distance of ~150 μm, the gradient becomes very steep, and consequently P_{pos} approaches 1.0, whereas the chemotaxis index increases slowly from 0.8 to 0.9 but never reaches the value of 1. These results suggest that in shallow gradients, the input signal for chemotaxis is closely related to P_{pos}.

The calculations presented in Fig. 2 reveal that different combinations of σ_B and I can explain the observed values of the chemotaxis index in the pipette assay. The chemotaxis data from the three different assays, exhibiting different gradient properties, were used to obtain experimental estimates for σ_B and I. For this, we assume $\Psi = P_{pos}$ and consider only the conditions with SNR < 0.7, by which $Erf[(\mathrm{SNR}/\sqrt{2}] \approx \sqrt{2/\pi}\mathrm{SNR}$. Thus the assumptions are $\Psi = \sqrt{2/\pi}$ SNR and $\Psi < 0.5$, and with these assumptions it holds that

$$\Psi = \frac{\frac{\Delta C R_t}{\sqrt{8\pi}K_D}}{\sqrt{\sigma_B^2 + \frac{CR_t}{K_D I}}}, \text{ or rewritten}$$

$$\left[\frac{\Delta C}{\Psi}\right]^2 = \frac{8\pi K_D}{R_t I} C + \frac{8\pi K_D^2}{R_t^2} \sigma_B^2. \quad (7)$$

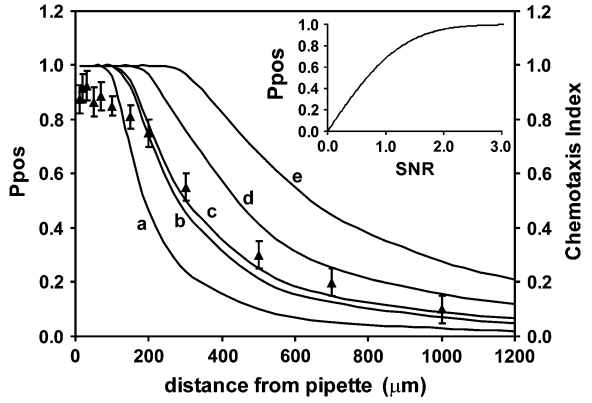

FIGURE 2 Measured chemotaxis index, and calculated P_{pos} at different distances from a micropipette containing 10^{-4} M cAMP. P_{pos} is the probability that the cell senses a gradient toward the pipette, and was calculated for different values of nonreceptor noise σ_B, sampling fold I, and receptor property R_t/K_D. (*a*) $\sigma_B = 100$, $I = 1$, $R_t/K_D = 400$; (*b*) $\sigma_B = 10$, $I = 1$, $R_t/K_D = 400$; (*c*) $\sigma_B = 0$, $I = 1$, $R_t/K_D = 400$; (*d*) $\sigma_B = 0$, $I = 3$, $R_t/K_D = 400$; or $\sigma_B = 0$, $I = 1$, $R_t/K_D = 1200$; (*e*) $\sigma_B = 0$, $I = 10$, $R_t/K_D = 400$; or $\sigma_B = 0$, $I = 1$, $R_t/K_D = 4000$. The measured chemotaxis index (▲) presents the means and standard deviations of at least three independent experiments. (*Inset*) P_{pos} calculated for different values of SNR.

A plot of $[\Delta C/\Psi]^2$ versus C will yield a straight line with slope $8\pi K_D/R_t I$ and intercept at the y axis of $(8\pi K_D^2/R_t^2)\sigma_B^2$. The experimental data for threshold chemotaxis from Table 1 ($\Psi = 0.2$), and all experimental data with $\Psi < 0.5$ are presented in Fig. 3. The data are described accurately by a straight line. From the slope, we calculated the sampling fold, yielding $I = 1.82$ (range 1.24–2.40; 95% confidence limit). The nonreceptor noise was calculated from the intercept with the ordinate, yielding $\sigma_B = 25.2$ (range 15.6–34.8). In this figure, we also plotted the calculated curve for $\sigma_B = 0$, which results in a significant less accurate fit of the experimental data.

Now that we have estimates of all parameters of SNR, we next investigated the relationship between the calculated P_{pos} and the chemotaxis index Ψ as measured in Fig. 1. Fig. 4 presents all observed chemotaxis data from the three assays as a function of the calculated P_{pos} using the appropriate equation for C and ΔC, all at $I = 1.8$ and $\sigma_B = 25$. The results show a remarkable close correlation between P_{pos} and Ψ for all assay conditions. The curve is linear with slope 1 at P_{pos} and Ψ below 0.5, and levels off to $\Psi = 0.8$ when P_{pos} approaches 1. The results strongly suggest that in shallow gradients, the chemotaxis index depends largely if not solely on P_{pos}, i.e., the probability that the half of the cell closer to the cAMP source receives a stronger receptor signal than the other half of the cell. Thus chemotaxis in shallow gradients is well described by a biased random walk.

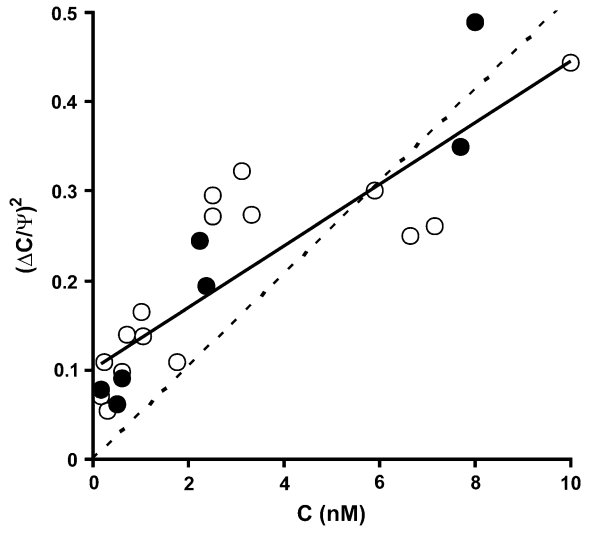

FIGURE 3 Plot of $[\Delta C/\Psi]^2$ versus C to derive estimates for nonreceptor noise σ_B and sampling fold I. The chemotaxis data of Fig. 1 and Table 1, and the corresponding values of the cAMP concentration C and spatial gradient ∇C were used. (*Solid symbols*) Chemotaxis data of Table 1 at $\Psi = 0.2$. (Open symbols) All measured chemotaxis data of Fig. 1 at $\Psi < 0.5$. Linear regression of all data yields $y = 0.0345x + 0.10$; $R^2 = 0.7423$. The slope is $8\pi K_D/R_t I$ and yields $I = 1.82$ (range 1.24–2.40; 95% confidence limits); the intercept with the ordinate is $(8\pi K_D^2/R_t^2)\sigma_B^2$ and yields $\sigma_B = 25.2$ (range 15.6–34.8). The dotted line is the linear regression for all data with $\sigma_B = 0$, yielding $y = 0.0516x$, $R^2 = 0.387$.

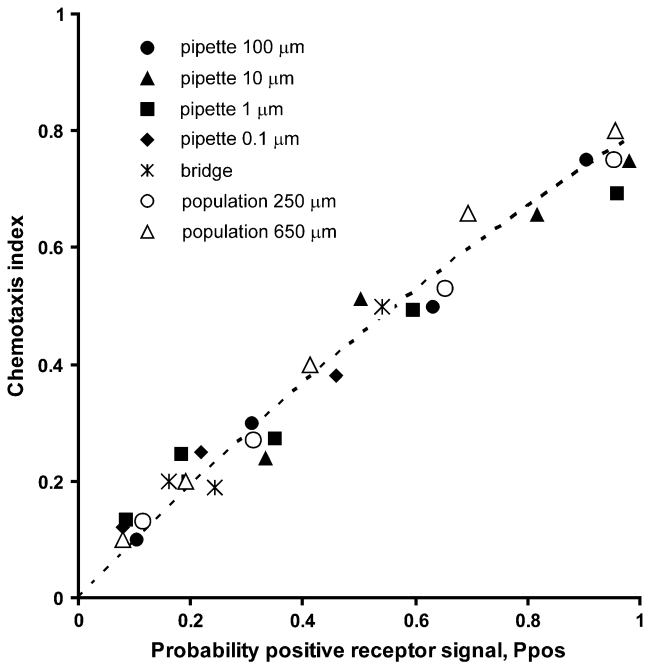

FIGURE 4 Chemotaxis index as function of P_{pos}. The chemotaxis index presented in Fig. 1 was determined with three assays using different experimental conditions. Equations A1–A6 were used to calculate the cAMP gradient around the cell in these assays, and Eqs. A8 and A9 were used to calculate P_{pos}, the probability that the cell senses a gradient toward the source of cAMP. The data are shown for $P_{pos} < 0.95$. In shallow gradients, when P_{pos} is small, the chemotaxis index is directly proportional to P_{pos}; in steeper gradients, chemotaxis reaches a maximum of $\Psi = 0.8$ when P_{pos} approaches 1. The dotted line is $\Psi = P_{pos}(1–0.2\ P_{pos})$.

DISCUSSION

Model for bias random walk

Dictyostelium cells in buffer extend a pseudopod on average every ~30 s; a pseudopod has a lifetime of ~60 s. We suppose that the time and place where a new pseudopod is made is regulated by activators and inhibitors in the cytoplasm. Alternatively, cells may extend a new pseudopod by splitting of an existing pseudopod, and one of the pseudopodia is stabilized and the other retracted (23), depending on the local balance between activators and inhibitors. We envision that cAMP receptor activation will influence the activity of one or multiple of these activators and inhibitors, thereby affecting the formation of new pseudopodia or stabilization of existing pseudopodia. In a shallow gradient of cAMP, this will result in a bias of the random formation of pseudopodia such that they are made more often in the direction of the gradient than in other directions. In such a probabilistic model for chemotaxis in very shallow gradients, there in no a priory need for gradient amplification steps.

P_{pos}, the probability to decipher a cAMP gradient

Dictyostelium cells are exquisitely sensitive to a spatial gradient of cAMP. At threshold chemotaxis ($\Psi = 0.2$), the minimal spatial gradient is ~5 pM/μm (Table 1), similar to what has been observed previously with the small population assay (3.6 pM/μm (8)) and microfluid devices (~3–5 pM/μm (24)). The difference in receptor occupancy between the two halves of the cell closest and farthest away from the cAMP source is only 5–10 occupied receptors per cell at threshold chemotaxis. We have analyzed chemotaxis in shallow gradients in the context of stochastic fluctuations of receptor occupancy, and derived an equation for P_{pos}, the probability that in a cAMP gradient the front half of the cell has higher receptor occupancy than the back half of the cell. We observed a very close correlation between the calculated P_{pos} values and the observed chemotaxis index. This close correlation was obtained with several different chemotaxis assays that depend either on the behavior of cell populations, or on the behavior of individual cells in stable spatial gradients or transient spatial gradients. These results suggest that the probability that a cell makes a new pseudopod or stabilizes an existing pseudopod in the direction of a shallow cAMP gradient depends on the probability that the cell has correctly determined the direction of the cAMP gradient.

P_{pos} depends on cAMP gradient, receptors, nonreceptor noise, and sampling time

The value of P_{pos} depends on four parameters: the cAMP gradient property$\Delta C/\sqrt{C}$, the receptor property R_t/K_D, the nonreceptor noise σ_B, and the sampling fold I. The observation that chemotaxis at low cAMP concentrations depends on $\Delta C/\sqrt{C}$ strongly supports the hypothesis that chemotaxis in shallow gradients is mediated by stochastic fluctuations of activated receptors. The $\sqrt{C}$ in the denominator is derived from the receptor noise, whereas ΔC in the nominator is derived from the signal: At low cAMP concentrations, the difference in receptor occupancy between the front and back of the cell is proportional to the absolute cAMP gradient ΔC (Eq. 1). The dependence of chemotaxis on $\Delta C/\sqrt{C}$ has been observed before in experiments in which the chemotaxis threshold was measured with increasing added background cAMP concentrations (9). The experiments were interpreted in the context of adaptation of the receptor to increasing background concentrations and not in the context of stochastic fluctuations of receptor occupancy. That interpretation is probably correct, because the applied background cAMP concentrations were very high (10^{-7}–10^{-5} M), essentially occupying all receptors unless the affinity of the receptors was changed by adaptation. These results suggest that chemotaxis depends on $\Delta C/\sqrt{C}$, both at low receptor occupancy, due to stochastic fluctuations of receptor occupancy, and at high receptor occupancy, due to adaptation mechanisms.

P_{pos}, and thus chemotaxis, is proportional to $\sqrt{I}$. The sampling fold I is the number of independent measurements of receptor occupancy, which depends on the sampling time T and the lifetime τ_R of the cAMP-receptor complex as described in Eq. 3. It is clear that chemotaxis will improve when the sampling fold I is large, which will be the case when the sampling time T is large or the lifetime τ_R of the cAMP-receptor complex is small. However, the consequence of a large sampling time T is that second messengers that transduce the signal will diffuse and lose spatial information. In addition, a very short lifetime τ_R of the cAMP-receptor complex will lead to a lower affinity of the receptor for cAMP, which reduces the sensitivity to detect low chemoattractant concentrations. Different kinetic forms of the receptor have been observed, for which the lifetimes τ_R of the active receptor have been obtained between 0.7 and 3.5 s (25,26). We derived the experimental value for sampling fold $I = 1.8$. From Eq. 3, we derive that $T/\tau_R = 2.1$, and therefore the sampling time T of the receptor/second messenger system is in the range of 1.5–7 s. It has been observed that *Dictyostelium* cells can extend a pseudopod in the direction of a micropipette with cAMP within ~5–10 s after application of the cAMP gradient (27–29). The importance of the sampling time for understanding the properties of the transducing second messenger will be discussed below.

The probability to detect a spatial gradient of chemoattractant is reduced by nonreceptor noise, σ_B. The source of nonreceptor noise can be a basal level of second messenger, fluctuations in the second messenger response, and fluctuations of the cAMP concentration in the vicinity of the receptor. We have not investigated the individual components that lead to nonreceptor noise. We obtained the experimental value for nonreceptor noise $\sigma_B = 25$. How does this value relate receptor noise σ_R? Equation 2 yields a receptor noise σ_R of 25 with $I = 1.8$ at $R^* = 347$ occupied receptors/cell,

which will occur at a cAMP concentration of ~1 nM. Thus, nonreceptor noise is very small, and above 1% occupancy of the receptors, the noise in the system is already dominated by receptor noise. This suggests that the second messenger system that mediates chemotaxis shows significant increases at very low cAMP concentrations, either because the system is fully activated at low receptor occupancy, or because basal levels of the second messenger are extremely low.

The transducing second messenger

We wish to deduce some general characteristics of a hypothetical second messenger M that transduces the signal from occupied chemoattractant receptors to activation of a pseudopodium in *Dictyostelium* and other systems. It is likely that the sampling time T is approximately equal to lifetime τ_M of the second messenger, i.e., $\tau_M = T$. It is clear that the sampling fold I can be large when the lifetime of the second messenger τ_M is large. However, to transduce the spatial information of occupied receptors to a local pseudopod, the second messenger should not diffuse too far from its place of production. On the other hand, mixing of second messenger molecules in the vicinity of their place of synthesis will reduce the temporal and spatial noise of the system. A molecule M that diffuses through a medium where it is degraded will have an average dispersal length l_M from the place of synthesis given by $l_M = \gamma\sqrt{D_M\tau_M}$, where γ is a constant that depends on the dimensions ($\gamma = 1$, $\pi/2$, and 2 for diffusion in one, two, or three dimensions, respectively) and D_M is the diffusion rate constant of M (30). Pseudopodia are protrusions of 2–4 μm in width. This suggests that the optimal dispersion length of M is between 1 and 3 μm. With these assumptions and $\gamma = 1.5$, it follows that $0.5 \le D_M\tau_M \le 5$. It is unlikely that the sampling time T and the lifetime of the second messenger τ_M are larger than the time that it takes for a cell to extend a pseudopod in the direction of the chemoattractant, which is 5–10 s in *Dictyostelium* (27–29) and 10–15 s in neutrophils (31,32), i.e., $3 \le \tau_M \le 20$. From this, it follows that $0.1 \le D_M \le 2$.

A second messenger that diffuses extremely slowly, such as transmembrane proteins ($\gamma = 1$, $D_m = 0.03$ $\mu m^2/s$ (11)), may have a very long lifetime τ_M up to 300 s before it diffuses outside the emerging pseudopod, and consequently the sampling fold I can be large (Fig. 5). However, diffusion is so slow that spatial integration of information over a distance of 1 μm would take several minutes and is essentially absent within the ~10 s time period that a cell extends a pseudopod toward a chemoattractant source. With a second messenger that diffuses somewhat faster, such as a phospholipid ($\gamma = 1.5$, $D_m = 1$ $\mu m^2/s$; (33,34)), spatial integration of the activity of multiple receptors will occur over a distance of 1 μm in ~0.5 s, and over a distance of the emerging pseudopod in ~4 s. In addition, the sampling fold I can be >1, provided that the receptor dissociates fast with a lifetime of <~3s. With a second messenger that diffuses still faster,

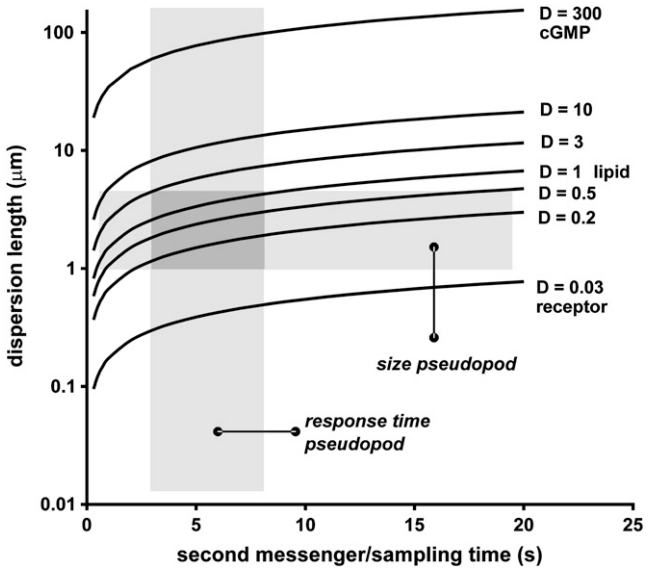

FIGURE 5 Dispersion length of diffusing second messengers as function of their lifetime and diffusion rate constant. The dispersion length of several potential second messengers was calculated with the equation $l_M = \gamma\sqrt{D_M\tau_M}$, where D_M is the diffusion rate constants (D, in $\mu m^2/s$), τ_M is the lifetime of the second messenger, and γ is between 1 and 2 depending on the dimension of diffusion ($\gamma = 1$, 1.5, and 2 for receptor, lipid, and cGMP, respectively). The shaded areas indicate the response time of a cell to extend a pseudopod in the direction of a new gradient (~3–8 s (27–29,31,32)), and the 1–3 μm size of a pseudopod, respectively. The intersection of these shaded areas suggests that the transducing second messenger has a diffusion rate constant of 0.2–2 $\mu m^2/s$.

such as soluble compounds like cAMP, cGMP, or IP3 ($\gamma = 2$, $D_m = 300$ $\mu m^2/s$ (35–37)), it is essentially impossible to retain spatial information, unless the lifetimes of the second messenger τ_M and the activated receptor τ_R are extremely short, in the order of 30 ms.

In conclusion, the optimal second messenger for chemotaxis in eukaryotes has a lifetime of 3–20 s and diffuses with a rate constant of ~1 $\mu m^2/s$. To obtain a sampling fold above 1, the chemoattractant should be detected by a receptor that has a lifetime of ~1 s. These properties allow for maximal temporal and spatial integration of activated receptors and minimal noise of stochastic receptor activation.

In *Dictyostelium*, the average lifetime of the cAMP-receptor complex τ_R is ~0.7–3.5 seconds (25,26); similar data have been obtained for the interaction between the fMLP and its receptor on human neutrophils, showing fMLP-receptor lifetimes between 0.5 and 3 s (38,39). Thus, the observed parameters for *Dictyostelium* are $I = 1.8$ (range 1.2–2.4) and $\tau_R = 0.7$–3.5 s, which yield a hypothetical second messenger with a lifetime of $\tau_M = 1.5$–7 s and a diffusion rate constant of $D_M = 0.25$–4 $\mu m^2/s$. The lifetime and diffusion rate constants of some potential second messengers have been measured. Although soluble second messengers such as cGMP and IP3 have the appropriate lifetime (40,41), they diffuse too fast (35–37). In contrast,

membrane-bound second messengers have generally slow diffusion (33,34) and some of them also short lifetimes (42). The best candidate is PIP3, which perfectly fits in the biophysical profile: very low basal levels resulting in low nonreceptor noise, rapid transient accumulation after cAMP stimulation with a half-life of ~5 s, and a diffusion rate constant of ~0.5 $\mu m^2/s$, resulting in a dispersion length of ~2.5 μm (7,33,34,42). It should be mentioned, however, that inhibition of PI3kinase has only moderate effects on chemotaxis in *Dictyostelium* (29,43–45), suggesting that other second messengers must be present that can take over the function of PIP3 in PI3kinase-null cells. Alternatives are the lipid products of PLC, PLA2, and PLD, or combinations of these enzymes, such as diacylglycerol, fatty acids (e.g., arachidonic acid) and lysophospholipids (e.g., lysophosphatidic acid).

APPENDIX

Equations A1–A6

When a pipette filled with cAMP is inserted in a field of *Dictyostelium* cells, cAMP will diffuse continuously from the pipette, leading a stable spatial gradient of which the concentration $C(x)$ and the spatial gradient $\nabla C(x)$ are dependent on the distance (x) from the pipette according to

$$C(x) = \frac{\alpha C_p}{x} \tag{A1}$$

and

$$\nabla C(x) = -\frac{\alpha C_p}{x^2}, \tag{A2}$$

where C_p is the cAMP concentration in the pipette and α is a proportionality constant that depends on the geometry of the pipette and the applied pressure; the experimentally observed value in our experiments is $\alpha = 0.05$ (see Materials and Methods). These equations are accurate descriptions of the cAMP gradient at a distance beyond 15 μm from the pipette; at shorter distances, more complex equations are required (M. Postma and P. J. M. van Haastert, unpublished).

In the modified Zigmond chamber, cells are deposited under a bridge. A cAMP gradient is formed by placing agar blocks with buffer on one side of the bridge and an agar block with cAMP on the other side (20). After a while, cells experience a gradient with the following properties (20):

$$C(x) = C_s\left(1 - \frac{x}{L}\right) \tag{A3}$$

and

$$\nabla C(x) = -\frac{C_s}{L}, \tag{A4}$$

where C_s is the cAMP concentration at the source, x is the distance from the source (700 μm), and L is the width of the bridge (2000 μm).

The small population assay scores the chemotactic response of a population of cells toward a cAMP source that has been applied at some distance away as a single dose. Due to diffusion in the agar, a transient cAMP gradient is formed that is maximal with the following properties (8):

$$C(x) = 0.49\frac{r^3}{x^3}C_d \tag{A5}$$

and

$$\nabla C(x) = 2.44\frac{r^3}{x^4}C_d, \tag{A6}$$

where r is the radius of the cAMP droplet (150 μm), x is the distance between cell population and cAMP source (250 or 650 μm), and C_d is the applied cAMP concentration in the droplet. Note in these equations the different order in x compared to the pipette assay, which is due to the single dose of cAMP in the small population assay compared to continuous release of cAMP from the pipette.

Equation A7

The difference in number of occupied receptors in the front half of the cell directed toward the gradient and the back half of the cell is given by

$$\Delta R^* = R_f^* - R_b^* = \frac{1}{2}R_t\frac{C + 1/4\Delta C}{C + 1/4\Delta C + K_D} - \frac{1}{2}R_t\frac{C - 1/4\Delta C}{C - 1/4\Delta C + K_D}. \tag{A7a}$$

We are interested in chemotaxis at low cAMP concentrations ($C \ll K_D$) in shallow gradients ($\Delta C \ll C$) for which it holds that $C + 1/4\Delta C + K_D$ and $C - 1/4\Delta C + K_D$ are approximately equal to $C + K_D$. Therefore Eq. A7a reduces to Eq. A7:

$$\Delta R^* = \frac{R_t}{4}\frac{\Delta C}{C + K_D}. \tag{A7}$$

Equations A8 and A9

We assume that cAMP-binding to the receptor is a simple bimolecular reaction with association rate k_1C and dissociation rate k_{-1}. The autocorrelation of the total receptor occupancy for lag time τ is given (46) by

$$A_{RR}(\tau) = R_t p_o p_u e^{-\frac{|\tau|}{\tau_R}}, \tag{A8a}$$

where R_t is the total number of receptors, $p_o = C/(C + K_D)$ denotes the fraction of occupied receptors, $p_u = K_D/(C + K_D)$ denotes the fraction of unoccupied receptors, and $\tau_R = 1/(k_1C + k_{-1})$ denotes the macroscopic time constant for the binding reaction. At zero lag time $\tau = 0$, the value of the autocorrelation function equals the variance of total receptor occupancy $\sigma^2_{R^*} = R_t p_o p_u$.

When the signal of occupied receptors is averaged over time, the filtered signal $R_F(t)$ is the convolution with an averaging filter $U(t)$ and the receptor occupancy $R^*(t)$:

$$R_F^*(t) = \int_{-\infty}^{\infty} R^*(s)U(s - t)ds, \tag{A8b}$$

where $U(t)$ is the rectangular filter with sampling time T:

$$U(t) = \frac{1}{T}\ |t| < \frac{T}{2}$$
$$U(t) = \frac{1}{2T}\ |t| = \frac{T}{2}$$
$$U(t) = 0\ |t| > \frac{T}{2}. \tag{A8c}$$

The autocorrelation function of the filter $U(t)$ is

$$A_{UU}(\tau) = \frac{T - |\tau|}{T^2}\ |\tau| < T$$
$$A_{UU}(\tau) = 0\ |\tau| \geq T. \tag{A8d}$$

The autocorrelation function of the filtered signal is then given by the convolution of the autocorrelation functions A_{RR} and A_{UU}:

$$A_{FF}(\tau) = \int_{-\infty}^{\infty} A_{RR}(s)A_{UU}(s-\tau)ds. \tag{A8e}$$

The variance of receptor occupancy $\sigma^2_{R^*_F}$ during a sampling time T is then given by the variance of the filtered signal:

$$\begin{aligned}\sigma^2_{R^*_F} &= \lim_{\tau\to 0} A_{FF}(\tau)\\ &= 2\int_0^T R_t p_o p_u e^{-\frac{s}{\tau_R}} \frac{T-s}{T^2} ds\\ &= R_t p_o p_u \frac{2\tau_R}{T}\left[1-\frac{\tau_R}{T}\left(1-e^{-\frac{T}{\tau_R}}\right)\right],\end{aligned} \tag{A8f}$$

which with $\sigma^2_{R^*} = R_t p_o p_u$ yields

$$\sigma^2_{R^*_F} = \frac{\sigma^2_{R^*}}{I}, \tag{A8g}$$

where

$$I = \frac{T}{2\tau_R}\left[1-\frac{\tau_R}{T}\left(1-e^{-\frac{T}{\tau_R}}\right)\right]^{-1}. \tag{A9}$$

Thus, the variance of total receptor occupancy after sampling $\sigma^2_{R^*_F}$ is the variance without sampling $\sigma^2_{R^*}$ divided by I, the sampling fold.

In our experiments, we are interested in the noise of the system in shallow gradients at low cAMP concentrations ($C \ll K_D$), which implies that $p_u = 1$ and thus $R_t p_o p_u = R^*$, and $\tau_R = 1/k_{-1}$, the lifetime of the cAMP-receptor complex. Therefore at low cAMP concentrations

$$\sigma^2_{R^*_F} = \frac{R^*}{I}. \tag{2}$$

REFERENCES

1. Baggiolini, M. 1998. Chemokines and leukocyte traffic. *Nature*. 392: 565–568.
2. Campbell, J. J., and E. C. Butcher. 2000. Chemokines in tissue-specific and microenvironment-specific lymphocyte homing. *Curr. Opin. Immunol.* 12:336–341.
3. Crone, S. A., and K. F. Lee. 2002. The bound leading the bound: target-derived receptors act as guidance cues. *Neuron*. 36:333–335.
4. Szurmant, H., and G. W. Ordal. 2004. Diversity in chemotaxis mechanisms among the bacteria and archaea. *Microbiol. Mol. Biol. Rev.* 68:301–319.
5. Wadhams, G. H., and J. P. Armitage. 2004. Making sense of it all: bacterial chemotaxis. *Nat. Rev. Mol. Cell Biol.* 5:1024–1037.
6. Devreotes, P., and C. Janetopoulos. 2003. Eukaryotic chemotaxis: distinctions between directional sensing and polarization. *J. Biol. Chem.* 278:20445–20448.
7. Postma, M., L. Bosgraaf, H. M. Loovers, and P. J. M. van Haastert. 2004. Chemotaxis: signalling modules join hands at front and tail. *EMBO Rep.* 5:35–40.
8. Mato, J. M., A. Losada, V. Nanjundiah, and T. M. Konijn. 1975. Signal input for a chemotactic response in the cellular slime mold *Dictyostelium discoideum*. *Proc. Natl. Acad. Sci. USA*. 72:4991–4993.
9. van Haastert, P. J. M. 1983. Sensory adaptation of *Dictyostelium discoideum* cells to chemotactic signals. *J. Cell Biol.* 96:1559–1565.
10. Xiao, Z., N. Zhang, D. B. Murphy, and P. N. Devreotes. 1997. Dynamic distribution of chemoattractant receptors in living cells during chemotaxis and persistent stimulation. *J. Cell Biol.* 139:365–374.
11. Ueda, M., Y. Sako, T. Tanaka, P. Devreotes, and T. Yanagida. 2001. Single-molecule analysis of chemotactic signaling in *Dictyostelium cells*. *Science*. 294:864–867.
12. Berg, H. C., and E. M. Purcell. 1977. Physics of chemoreception. *Biophys. J.* 20:193–219.
13. Bialek, W., and S. Setayeshgar. 2005. Physical limits to biochemical signaling. *Proc. Natl. Acad. Sci. USA*. 102:10040–10045.
14. Arrieumerlou, C., and T. Meyer. 2005. A local coupling model and compass parameter for eukaryotic chemotaxis. *Dev. Cell*. 8:215–227.
15. Moghe, P. V., and R. T. Tranquillo. 1994. Stochastic model of chemoattractant receptor dynamics in leukocyte chemosensory movement. *Bull. Math. Biol.* 56:1041–1093.
16. Tranquillo, R. T., D. A. Lauffenburger, and S. H. Zigmond. 1988. A stochastic model for leukocyte random motility and chemotaxis based on receptor binding fluctuations. *J. Cell Biol.* 106:303–309.
17. Fisher, P. R., R. Merkl, and G. Gerisch. 1989. Quantitative analysis of cell motility and chemotaxis in *Dictyostelium discoideum* by using an image processing system and a novel chemotaxis chamber providing stationary chemical gradients. *J. Cell Biol.* 108:973–984.
18. Fisher, P. R. 1990. Pseudopodium activation and inhibition signals in chemotaxis by *Dictyostelium discoideum* amoebae. *Semin. Cell Biol.* 1:87–97.
19. Soll, D. R., D. Wessels, P. J. Heid, and H. Zhang. 2002. A contextual framework for characterizing motility and chemotaxis mutants in *Dictyostelium discoideum*. *J. Muscle Res. Cell Motil.* 23:659–672.
20. Veltman, D. M., and P. J. van Haastert. 2006. Guanylyl cyclase protein and cGMP product independently control front and back of chemotaxing *Dictyostelium* cells. *Mol. Biol. Cell*. 17:3921–3929.
21. Konijn, T. M. 1970. Microbiological assay for cyclic 3′,5′-AMP. *Experientia*. 26:367–369.
22. Soll, D. R. 1999. Computer-assisted three-dimensional reconstruction and motion analysis of living, crawling cells. *Comput. Med. Imaging Graph.* 23:3–14.
23. Andrew, N., and R. H. Insall. 2007. Chemotaxis in shallow gradients is mediated independently of PtdIns 3-kinase by biased choices between random protrusions. *Nat. Cell Biol.* 9:193–200.
24. Song, L., S. M. Nadkarni, H. U. Bodeker, C. Beta, A. Bae, C. Franck, W. J. Rappel, W. F. Loomis, and E. Bodenschatz. 2006. *Dictyostelium discoideum* chemotaxis: threshold for directed motion. *Eur. J. Cell Biol.* 85:981–989.
25. van Haastert, P. J. M., and R. J. De Wit. 1984. Demonstration of receptor heterogeneity and affinity modulation by nonequilibrium binding experiments. The cell surface cAMP receptor of *Dictyostelium discoideum*. *J. Biol. Chem.* 259:13321–13328.
26. van Haastert, P. J. M., R. J. de Wit, P. M. W. Janssens, F. Kesbeke, and J. DeGoede. 1986. G-protein-mediated interconversions of cell-surface cAMP receptors and their involvement in excitation and desensitization of guanylate cyclase in *Dictyostelium discoideum*. *J. Biol. Chem.* 261:6904–6911.
27. Gerisch, G., D. Hulser, D. Malchow, and U. Wick. 1975. Cell communication by periodic cyclic-AMP pulses. *Phil. Trans. R. Soc. London. B*. 272:181–192.
28. Swanson, J. A., and D. L. Taylor. 1982. Local and spatially coordinated movements in *Dictyostelium discoideum* amoebae during chemotaxis. *Cell*. 28:225–232.
29. Postma, M., J. Roelofs, J. Goedhart, H. M. Loovers, A. J. W. G. Visser, and P. J. M. van Haastert. 2004. Sensitization of *Dictyostelium* chemotaxis by PI3-kinase mediated self-organizing signalling patches. *J. Cell Sci.* 117:2925–2935.
30. Postma, M., and P. J. M. van Haastert. 2001. A diffusion-translocation model for gradient sensing by chemotactic cells. *Biophys. J.* 81:1314–1323.
31. Shelve, D. V., A. M. Alterative, and D. Chodniewicz. 2004. Controlled pseudopod extension of human neutrophils stimulated with different chemoattractants. *Biophys. J.* 87:688–695.

32. Gerisch, G., and H. U. Keller. 1981. Chemotactic reorientation of granulocytes stimulated with micropipettes containing fMet-Leu-Phe. *J. Cell Sci.* 52:1–10.

33. Almeida, P. F. F., and W. L. C. Vaz. 1995. Lateral Diffusion in Membranes. Elsevier, Amsterdam.

34. Haugh, J. M., F. Codazzi, M. Teruel, and T. Meyer. 2000. Spatial sensing in fibroblasts mediated by 3′ phosphoinositides. *J. Cell Biol.* 151:1269–1280.

35. Chen, C., T. Nakamura, and Y. Koutalos. 1999. Cyclic AMP diffusion coefficient in frog olfactory cilia. *Biophys. J.* 76:2861–2867.

36. Tsaneva-Atanasova, K., D. I. Yule, and J. Sneyd. 2005. Calcium oscillations in a triplet of pancreatic acinar cells. *Biophys. J.* 88:1535–1551.

37. Hofer, T., L. Venance, and C. Giaume. 2002. Control and plasticity of intercellular calcium waves in astrocytes: a modeling approach. *J. Neurosci.* 22:4850–4859.

38. Hoffman, J. F., J. J. Linderman, and G. M. Omann. 1996. Receptor up-regulation, internalization, and interconverting receptor states. Critical components of a quantitative description of *N*-formyl peptide-receptor dynamics in the neutrophil. *J. Biol. Chem.* 271:18394–18404.

39. Sklar, L. A., H. Mueller, G. Omann, and Z. Oades. 1989. Three states for the formyl peptide receptor on intact cells. *J. Biol. Chem.* 264: 8483–8486.

40. van Haastert, P. J. M., and P. R. van der Heijden. 1983. Excitation adaptation and deadaptation of the cAMP mediated cGMP response in *Dictyostelium discoideum*. *J. Cell Biol.* 96:347–353.

41. van Haastert, P. J. M., M. J. de Vries, L. C. Penning, F. Roovers, J. van der Kaay, C. Erneux, and M. M. van Lookeren Campagne. 1989. Chemoattractant and guanosine 5′-[gamma-thio]triphosphate induce the accumulation of inositol 1,4,5,-trisphophate in *Dictyostelium* cells that are labelled with [3H] inositol by electroporation. *Biochem. J.* 258:577–586.

42. Huang, Y. E., M. Iijima, C. A. Parent, S. Funamoto, R. A. Firtel, and P. N. Devreotes. 2003. Receptor mediated regulation of PI3Ks confines PI(3,4,5)P3 to the leading edge of chemotaxing cells. *Mol. Biol. Cell.* 14:1913–1922.

43. Funamoto, S., R. Meili, S. Lee, L. Parry, and R. A. Firtel. 2002. Spatial and temporal regulation of 3-phosphoinositides by PI 3-kinase and PTEN mediates chemotaxis. *Cell.* 109:611–623.

44. Iijima, M., and P. Devreotes. 2002. Tumor suppressor PTEN mediates sensing of chemoattractant gradients. *Cell.* 109:599–610.

45. Loovers, H., M. Postma, I. Keizer-Gunnink, Y. E. Huang, P. N. Devreotes, and P. J. M. Van Haastert. 2006. Distinct roles of PI(3,4,5)P3 during chemoattractant signaling in *Dictyostelium*: a quantitative in vivo analysis by inhibition of PI3-kinase. *Mol. Biol. Cell.* 17:1503–1513.

46. Colquhoun, D., and A. G. Hawkes. 1977. Relaxation and fluctuations of membrane currents that flow through drug-operated channels. *Proc. R. Soc. Lond. B Biol. Sci.* 199:231–262.